

AN ABSTRACT OF THE THESIS OF

Evan F. DeBlander for the degree of Honors Baccalaureate of Science
in Engineering Physics presented on May 22, 2009.

Title: Characterization of BaCuSF Thin Films Grown in Excess Copper, by Pulsed Laser
Deposition

Abstract approved: _____

Janet Tate

Thin films of the *p*-type semiconductor, barium copper sulfide fluoride (BaCuSF) were deposited using pulsed laser deposition. Similar *p*-type conductivity in Cu₂O is caused by copper vacancies. Addition of copper dopant is proposed as a method for filling the copper vacancies in BaCuSF. The films are characterized to determine quality using x-ray diffraction (XRD), atomic force microscopy (AFM), optical absorption, Seebeck, and resistivity measurements. The optimal deposition parameters with no added copper are: substrate temperature of 525 °C, argon gas pressure of 10⁻⁵ Torr, target-substrate distance of 2 inches, and a pulse repetition rate of 3 Hz. Copper is added to films produced at optimal deposition parameters at pulse ratios of 1000:1000 to 12:1000. Resistivity measurements are compared with theoretical copper content of the film to determine the success of the dopant. The film produced with a pulse ratio of 40:1000 has the closest to stoichiometric copper as well as the highest resistivity. This corresponds well with the filling of copper vacancies.

Keywords: BaCuSF, PLD, pulsed laser deposition, copper vacancies, *p*-type
semiconductor

Corresponding e-mail address: deblande@onid.orst.edu

©Copyright by Evan F. DeBlander
May 22, 2009
All Rights Reserved

Characterization of BaCuSF Thin Films Grown
in Excess Copper, by Pulsed Laser Deposition

by

Evan F. DeBlander

A PROJECT

submitted to

Oregon State University

University Honors College

in partial fulfillment of
the requirements for the
degree of

Honors Baccalaureate of Science in Engineering Physics

Presented May 22, 2009

Commencement June 2009

Honors Baccalaureate of Science in Engineering Physics

project of Evan F. DeBlander presented on May 22, 2009.

APPROVED:

Mentor, representing Physics

Committee Member, representing Physics

Committee Member, representing Materials Science

Chair, Department of Physics

Dean, University Honors College

I understand that my project will become part of the permanent collection of Oregon State University, University Honors College. My signature below authorizes release of my project to any reader upon request.

Evan F. DeBlander, Author

ACKNOWLEDGEMENTS

I would like to thank Janet Tate for offering me the opportunity to work in her lab. I would also like to thank her for all her guidance, insight, and patience in helping me complete this project. I would like to thank Andriy Zakutayev for all of his work on the project, as well as all of the help he gave me in making sense of the data. I would like to thank Morgan Emerson for her help in taking data as well. I would also like to thank Brady Gibbons for getting my writing skills to where they needed to be in order to start this thesis.

I would like to thank the Oregon State University Honors College, without them I would not have pushed myself to do the extra work required in a thesis. Finally I would like to thank all my friends and family who pushed me to excel in school.

TABLE OF CONTENTS

1. INTRODUCTION.....	1
2. CHARACTERIZATION TECHNIQUES.....	6
2.1 Structural Measurements	6
2.2 Optical Measurements	10
2.3 Transport Measurements	12
3. PULSED LASER DEPOSITION PARAMETERS	18
3.1 Substrate Temperature.....	20
3.2 Target-Substrate Distance	23
3.3 Repetition Rate	24
3.4 Background Gas Pressure.....	26
4. COPPER DOPING	28
5. CONCLUSION	34
6. BIBLIOGRAPHY	36

LIST OF FIGURES

<u>Figure</u>	<u>Page</u>
Figure 1-1: Band gap diagram for n-type and p-type semiconductors.	2
Figure 1-2: Crystalline structure of ideal BaCuSF.	4
Figure 2-1: Phase diagrams showing the formation energies of different impurities, the experimental results show either BaS, BaF ₂ , or both.....	8
Figure 2-2: XRD taken on BaCuSF thin films deposited with different Argon pressures. The sample deposited at 10 ⁻⁸ Torr had no added argon during the deposition in the chamber.....	9
Figure 2-3: Atomic force microscopy of BaCuSF film without extra copper, deposited at optimal deposition parameters.	10
Figure 2-4: Optical absorption in BaCuSF thin films deposited at with different Ar background pressures.....	12
Figure 2-5: a.) Example of Van der Pauw basic contact configuration. b.) Preferred contact configuration. c.) Contact configuration used in resistivity measurements.	14
Figure 2-6: Simple method for determining the characteristic resistances of a thin sample.	15
Figure 2-7: Resistivity of BaCuSF thin films deposited at different substrate temperatures.....	16
Figure 2-8: Seebeck coefficient measured at different substrate temperatures.	18
Figure 3-1: Pulsed laser deposition system.....	19
Figure 3-2: Optical absorption graphs of BaCuSF formed at different substrate temperatures. For easier viewing the graphs have been offset vertically.	21
Figure 3-3: X-ray diffraction patterns of BaCuSF films formed at different substrate temperatures. The XRD powder spectra of BaCuSF, BaF ₂ , and BaS are shown for comparison.....	22
Figure 3-4: X-ray diffraction patterns of BaCuSF films formed at different target-substrate distances. The XRD powder spectra of BaCuSF, BaF ₂ , and BaS are shown for comparison.	24
Figure 3-5: X-ray diffraction patterns of BaCuSF films formed using different laser repetition rates.....	25
Figure 3-6: Optical absorption graphs of BaCuSF formed at varying laser repetition rates. The graphs have been offset vertically.	26
Figure 3-7: X-ray diffraction patterns of BaCuSF films formed using different background gas pressures.	27
Figure 3-8: Optical absorption graphs of BaCuSF formed at varying background gas pressures, at 525°C substrate temperature,	28

Figure 4-1: Amount of excess copper present in films of BaCuSF. Amount is extrapolated from previous EPMA data gathered on BaCuTeF.	29
Figure 4-2: XRD results for BaCuSF films doped with various amounts of excess copper, deposited using optimal parameters. The samples with 12 and 40 pulses were measured significantly later than the other films.	31
Figure 4-3: Optical absorption in BaCuSF thin films with varying amounts of added copper, deposited using optimal parameters.	32
Figure 4-4: Resistivity measured for varying amounts of added copper.	33

Characterization of BaCuSF Thin Films Grown in Excess Copper, by Pulsed Laser Deposition

1. INTRODUCTION

Semiconductors are unique materials that have conductivity intermediate between metals and insulators. This conductivity relies mainly on defects present in the material and is very sensitive to defect concentration. The process of adding defects to a semiconductor in a controlled manner is called doping. A primary goal of semiconductor research is to understand the origin and behavior of dopants. The goal of this thesis is to characterize BaCuSF thin films grown in excess copper. This excess copper can act as a dopant in the material and allow for control over the conductivity. BaCuSF is a known *p*-type semiconductor, which is interesting because the *p*-type conductivity occurs in combination with a wide band gap.¹ A band gap larger than 3 eV, which is present in BaCuSF, allows the transmission of visible light.

Defects come in several forms, defects that accept an electron, called acceptors, defects that donate an electron, called donors, and neutral defects. A donor is a defect which has an extra electron. Since this electron is not bonded as strongly to its surrounding atoms, less energy is required to excite it into the conduction band. With an applied voltage the electrons that have been excited into the conduction band contribute to the conductivity of the material. When the conductivity contribution comes primarily from a donor, it is called *n*-type. Conversely, an acceptor is a defect in the material which is missing an electron. A hole is created when an electron from the valence band moves into this defect. Under an applied voltage the hole will progress through the

material in the direction of increasing voltage. When the contribution to conductivity comes primarily from acceptor impurities, the majority charge carriers are positively charged holes, and the material is called *p*-type. Figure 1-1 shows an energy diagram of both *p*-type and *n*-type semiconductors.

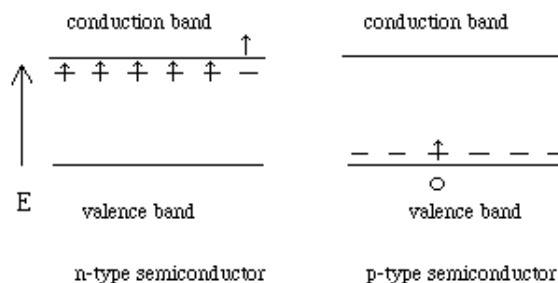


Figure 1-1: Band gap diagram for n-type and p-type semiconductors.²

Figure 1-1 shows that the energy required to promote an electron from the defect level into the conduction band is much less than what is required to promote an electron from the valence band to the conduction band. This is also true for promoting an electron from the valence band into an acceptor state, leaving behind a mobile hole.

The nature of the defects can vary greatly between different materials. In the well known semiconductor, silicon, *n*-type conductivity can be induced by doping the material with phosphorus. Phosphorus has five valence electrons, one more than silicon. When phosphorus is added to silicon it acts as a donor because the extra valence electron forms a defect state below the conduction band. *P*-type conductivity results from doping silicon with boron, which has three valence electrons. In this configuration boron acts as an acceptor.

In BaCuSF *p*-type conductivity is observed.¹ This *p*-type behavior is thought to be caused by copper vacancies.³ A copper vacancy occurs when a site in the crystal

lattice which should contain a copper atom is left unoccupied. The copper in this material is expected to be present as Cu^{1+} . Copper has a full d orbital which exists as the closed shell, and one additional electron which is above this shell ($3d^{10}4s^1$). This extra electron is easily lost, leaving Cu^{1+} with a full electronic shell ($3d^{10}4s^0$). When a copper vacancy is present, the overall material loses this extra electron, creating a hole in one of the bonds. This hole can be thermally excited into the valence band and cause an increase in carrier concentration, and conductivity.

BaCuSF is made up of alternating layers of CuS, and BaF which bond together in a way that can be seen in Figure 1-2. Many of these layers bonded together form the film.⁴ This structure will lead to higher conductivity parallel to the layers of material.⁴ Cu_2S is a known p-type semiconductor with a band gap of 1.2 eV, while BaF is an insulator with a wide band gap of 10.6.⁵ The mechanism that leads to semiconductor behavior in Cu_2S is also thought to be caused by copper vacancies.³ Copper vacancies could also be causing conductivity in the layers of CuS present in BaCuSF.

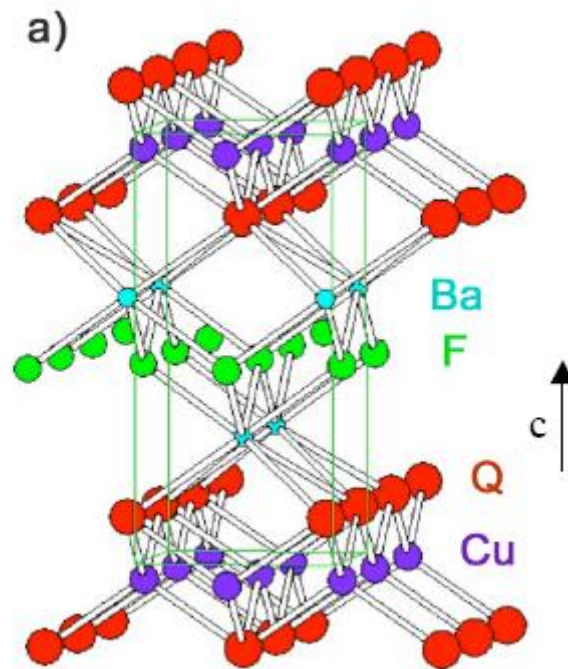


Figure 1-2: Crystalline structure of ideal BaCuSF.⁶

These copper vacancies are found in Cu_2O because the formation energy of a copper vacancy is lower than that of other potential acceptors.³ The formation energy for a copper vacancy ranges from 0.7 eV in a copper rich environment, to 0.5 eV for a copper poor environment. The formation energy of oxygen interstitial, which is the other potential cause for *p*-type behavior, ranges from 1 eV to 1.75 eV.³ Due to similarities between oxygen and sulfur it can be expected that the Cu_2S layers found in BaCuSF will behave much like Cu_2O . This will lead to copper vacancies created in a similar way to that found for Cu_2O .

When dealing with semiconductors such as BaCuSF, it is desirable to control the conductivity in the material by varying the amount of dopants. In a pure BaCuSF crystal only the intrinsic conductivity of the material would be present. With the large expected band gap of this material, more than 3 eV, the intrinsic conductivity is expected to be

very low. It can be found experimentally that thin films created with stoichiometric targets of BaCuSF have conductivity higher than what is intrinsically expected. In BaCuSF the intrinsic conductivity is negligible, as its band gap is well within the insulator range. This must be caused by some change in the stoichiometry of the film. In this paper it is proposed that this additional *p*-type conductivity is caused by copper vacancies in the material. By doping the films with additional copper, this conductivity should be reduced to near the intrinsic level. The expected result is that the conductivity will decrease from some preset level as additional copper is introduced. This conductivity will reach its lowest value near the intrinsic level. After passing this point, all copper vacancies will have been filled. The film will again be non-stoichiometric. Any copper added after this point will lead to the addition of new impurities. It will be possible to measure the number of holes present based on the Hall coefficient.

All thin films were fabricated by pulsed laser deposition (PLD). The basic idea is to place a target of the desired material into a vacuum chamber, and irradiate it with short laser pulses, depositing material onto a SiO₂ substrate in the process. With enough laser pulses, a film of the desired thickness is created. Copper is introduced in the films by intermittently adding layers of copper from a second copper target. It is expected that the extra copper diffuses throughout the film, filling copper vacancies in the crystal lattice. This paper discusses the characterization of BaCuSF films with extra copper by x-ray diffraction, atomic force microscopy, optical absorption, resistivity and Seebeck. The effect of various PLD parameters is explored and the effect of the inclusion of extra copper is investigated.

2. CHARACTERIZATION TECHNIQUES

Thin films of BaCuSF are produced by pulsed laser deposition. The deposition parameters are varied in order to produce films of the highest quality. The quality of the films is characterized by taking a series of different measurements. The measurements are broken into three different categories. The first category refers to those measurements which directly measure the structure of the films. This category consists of X-ray diffraction (XRD) and atomic force microscopy (AFM). In the case of AFM the surface structure of the film is measured directly. XRD uses the patterns of x-rays scattered off the material to infer crystal structure.

The next category contains all optical measurements; these include reflection and transmission data, which are used to determine the absorption of the film. The last category is the transport properties. The transport measurements determine the resistivity. They also provide data on the exact nature of this resistivity by providing carrier concentration and mobility information.

2.1 Structural Measurements

The structural measurements are done to verify that the film has formed in the expected manner. It is expected that the material will have the crystal structure shown in Figure 1-2, with no impurities. The film is not expected to grow into a single crystal. Small chunks of single crystals, called grains, can be expected. The grain size will affect other properties. X-ray diffraction is used to find the purity of the film, while atomic force microscopy is used in order to find the size of the grains.

2.1.1 X-ray Diffraction

The first test run on a sample is X-ray diffraction. X-ray diffraction is a method for determining the chemical composition and crystallinity of the samples. Every crystalline structure corresponds to a unique X-ray diffraction fingerprint. By comparing the XRD pattern for each sample to one that corresponds to pure BaCuSF, the relative purity of each sample can be determined. Each peak in the diffraction pattern corresponds with some plane in the geometry of the sample. The width of these peaks can be used to determine how uniform the crystal structure is. A sharp, narrow peak would correspond with a very well formed crystal, whereas a broad peak would correspond to poorly crystallized material.

Any additional peaks are compared with the different expected impurities of the material. The expected impurities follow the phase diagrams seen in Figure 2-1. In the films of BaCuSF produced, these phases were BaF₂, BaS, or both. This would suggest that either the samples were produced in a Barium or Fluorine rich environment, or a copper poor environment.

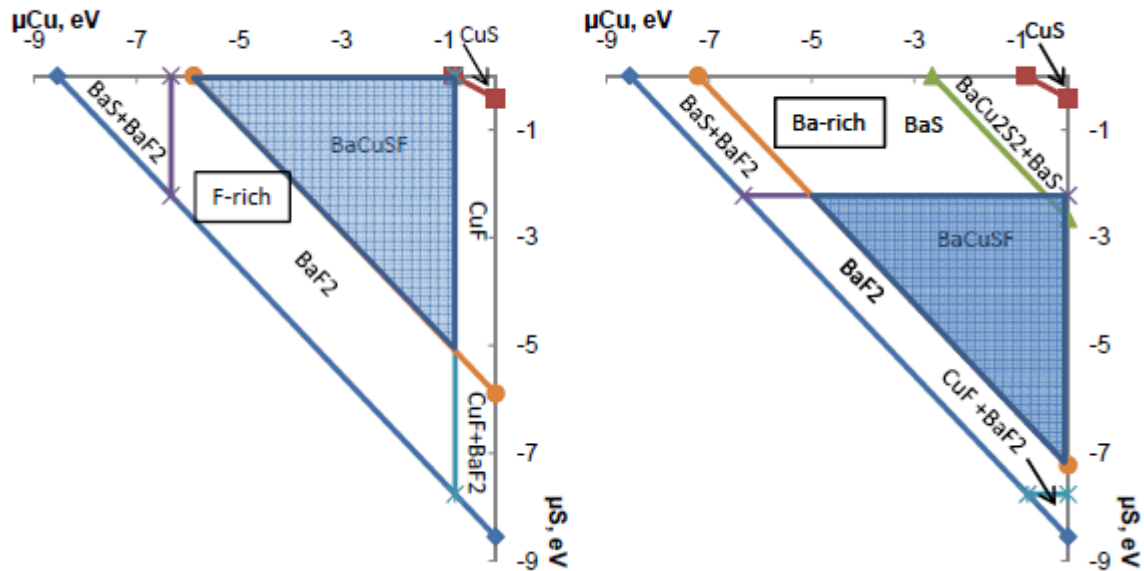


Figure 2-1: Phase diagrams showing the formation energies of different impurities, the experimental results show either BaS, BaF₂, or both.⁷

Ideally a sample would consist of only those peaks corresponding to the reference pattern. This did not always occur and the sample with the smallest and least defined impurity peaks was usually selected for additional characterization. An example of an X-ray diffraction measurement is shown in Figure 2-2. The sample produced at 10^{-5} Torr argon atmosphere in has the sharpest peaks corresponding to BaCuSF, and only small peaks corresponding to BaF₂. This sample has the best XRD characteristics.

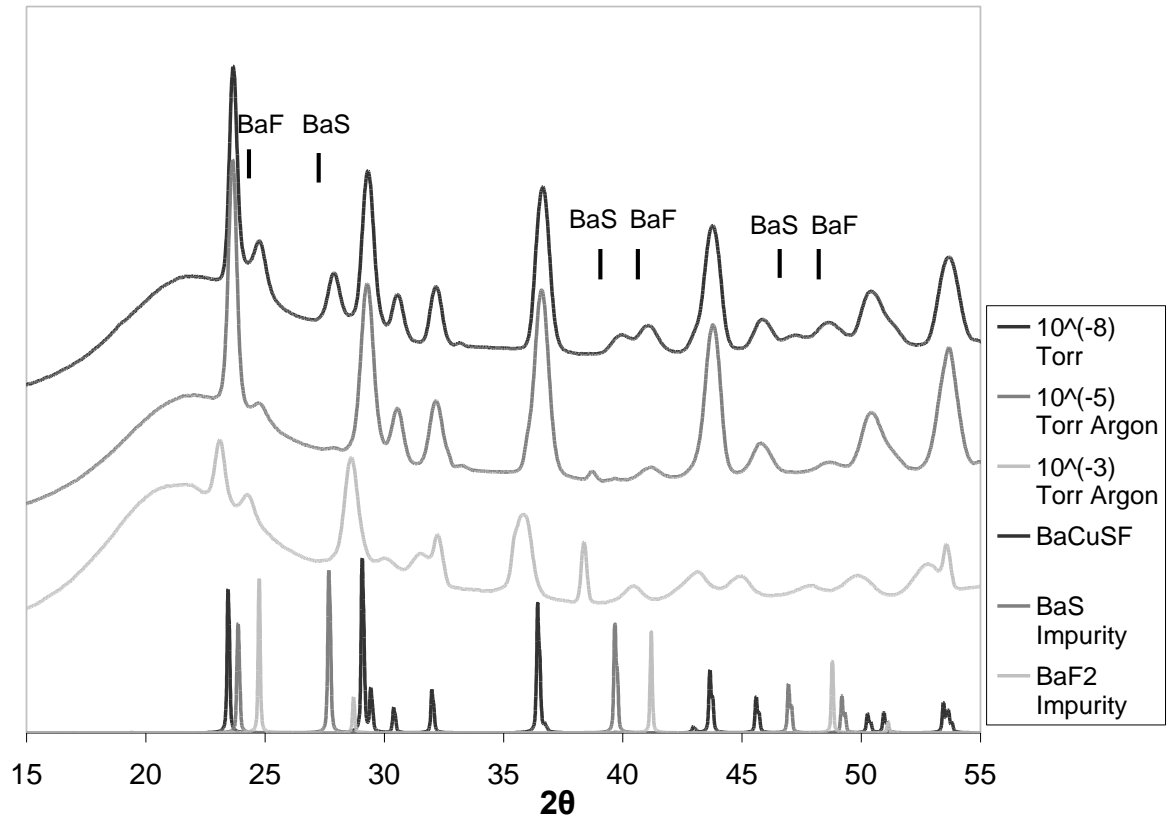


Figure 2-2: XRD taken on BaCuSF thin films deposited with different Argon pressures. The sample deposited at 10^{-8} Torr had no added argon during the deposition in the chamber.

2.1.2 Atomic Force Microscopy

This measurement uses a tiny cantilevered probe to measure the height of the sample. The probe has a small tip on the end which comes in very close contact with the surface of the film. The probe is then dragged across the surface of the sample, higher regions of the sample result in a larger atomic force being exerted on the tip. This increased force deflects the probe upwards. Any deflections in the probe are measured using an optical system which reflects laser light off of the probe. The grains can be seen in Figure 2-3.

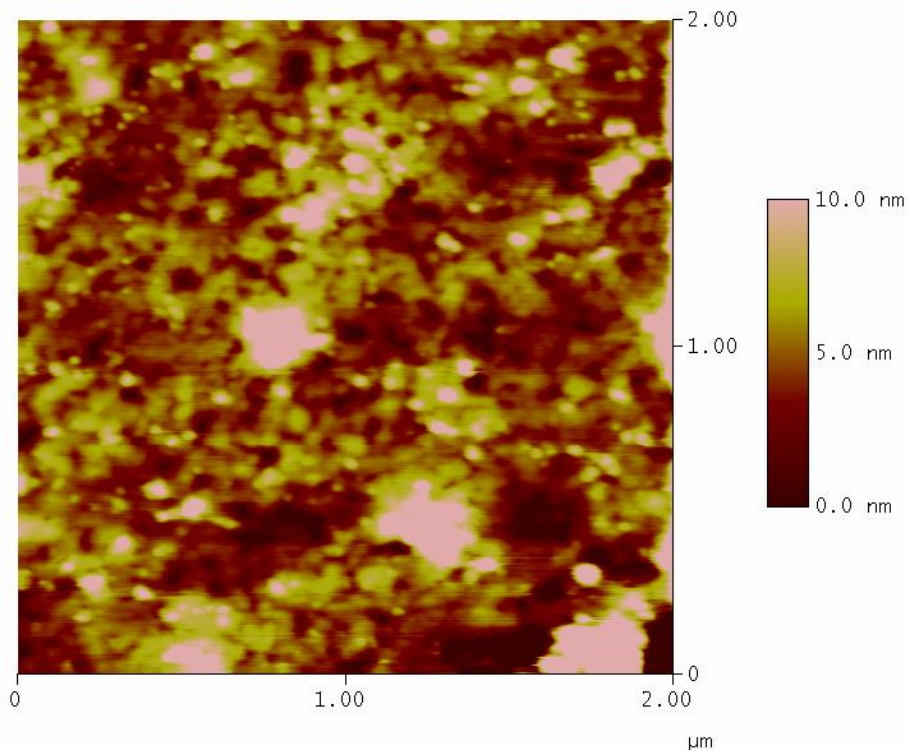


Figure 2-3: Atomic force microscopy of BaCuSF film without extra copper, deposited at optimal deposition parameters.

The grains can be seen as the regions with a similar height, or as seen in the figure, a uniform color. The grain size can greatly affect the transport properties of the material. Scattering that occurs at the grain boundaries lowers the conductivity of the films.

2.2 Optical Measurements

The optical measurements confirm the crystalline structure of the films, as well as provide a quantitative method for measuring film quality. Measurements are taken on each individual sample. First the sample is mounted onto an optical stand. This stand is placed in the path of a beam of incident light with a known intensity. A detector is placed behind the sample in order to measure the transmission intensity of the sample.

The transmission is measured as the incident radiation is changed in wavelength. Then the detector is placed at a position to gather reflected like, this data is also gathered for the same range of different wavelengths. These measurements along with the incident intensity are used to find the reflectance R , and the transmittance T , this is done using the following equations: $T = I_t/I_o$, $R = I_r/I_o$ where I_o is the incident irradiance, I_t is the transmitted and I_r is the reflected irradiance.⁸ This information is then used to calculate the

absorption coefficient of the film using the following equation: $\alpha = \frac{-\ln\left(\frac{T}{1-R}\right)}{d}$ where d is the thickness. The band gap of the material can be determined from the point in the material where the absorption increases greatly, this is seen at around 3.45 eV in Figure 2-4. The sharpness with which the absorption increases around the band gap is a good indicator of the quality of the film. This is because poor quality films have impurity states that fall below the band gap.

Another good indicator of film quality is the excitonic peak. An exciton is a quasiparticle made up of an electron bound to a hole. An exciton can be created when an electron from the valence band is excited into the conduction band, leaving behind a hole. Since the electron and hole are bound together, their energy is slightly less than it would be if they were unbound. This is similar to the binding of an electron and a proton. The creation of excitons allows for optical absorption to occur slightly below the band gap energy. The sharpness with which these peaks in absorption can be resolved can be used to infer the relative quality between similar films. In Figure 2-4 the film deposited at 1^{-5} Torr exhibits the sharpest excitonic peak, this deposition parameter ended up being chosen as an optimal parameter.

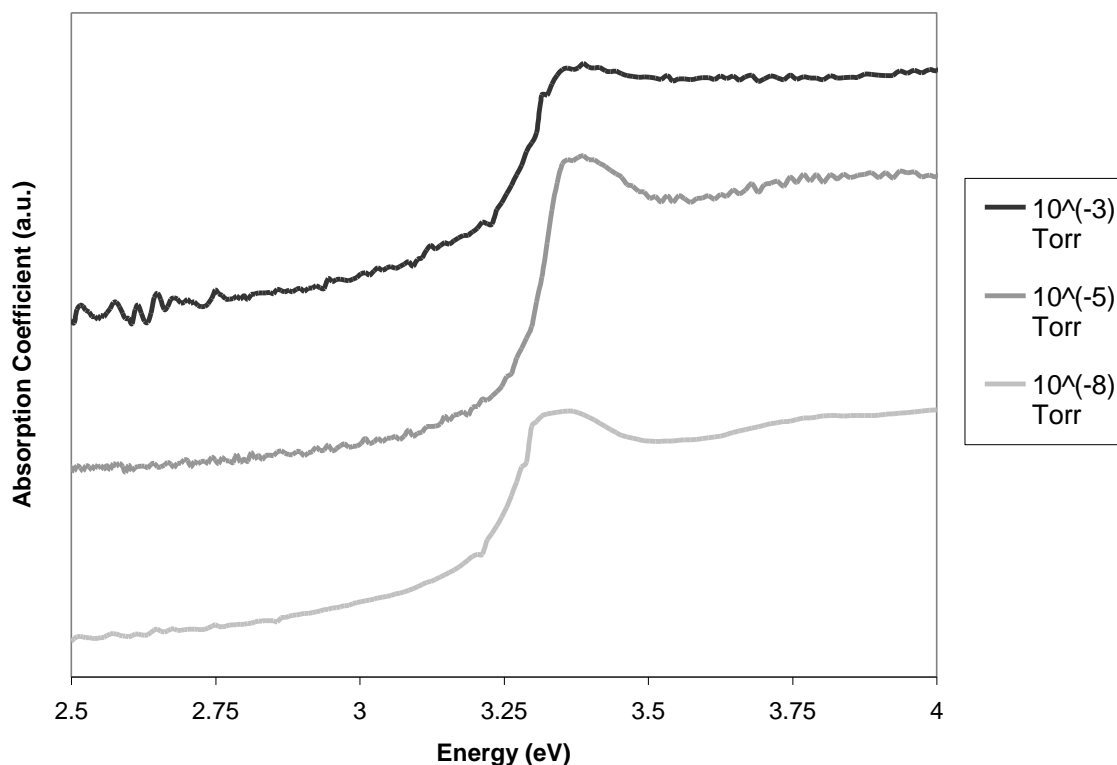


Figure 2-4: Optical absorption in BaCuSF thin films deposited at 525°C with different Ar background pressures.

2.3 Transport Measurements

The transport measurements consist of Hall measurements and Seebeck measurements. The Hall measurements determine the resistivity of the material as well as the carrier concentration, and hall mobility. The success of the doping process can be found from the resistivity measurement, with high resistivity values indicating a stoichiometric sample. The carrier concentration determines how many carriers are present in the material, since this material is expected to be *p*-type, the carriers are expected to be holes. The mobility of the sample gives a measure for how well carriers present in that material can move. This relates to the rate of scattering, collision, and other phenomena that affect the motion of a carrier. The carrier concentration and

mobility measurements were taken for the samples, however due to the high resistivity of the samples the data were not meaningful. This data was collected along with the resistivity measurements as discussed below.

The Seebeck measurement measures the electrical response of the film to an applied temperature gradient.

2.3.1 Resistivity

The resistivity of the samples was calculated using the Van der Pauw method. This method is commonly used in the electrical characterization of thin films, and the resistivity, mobility, and carrier concentration can be obtained from the same setup. The basic concept is that four contacts are made around the edge of the sample, as seen in Figure 2-5.

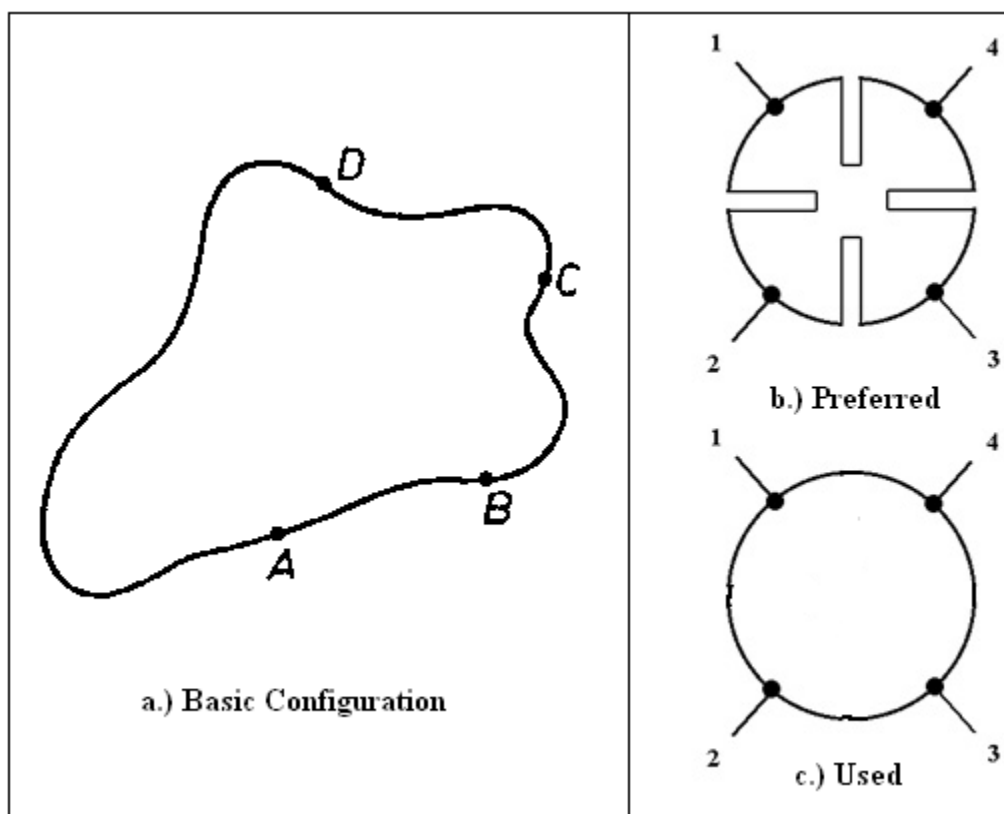


Figure 2-5: a.) Example of Van der Pauw basic contact configuration. b.) Preferred contact configuration. c.) Contact configuration used in resistivity measurements.⁹

In the samples of BaCuSF these contacts were made around a circle. This method was used because some samples had very high resistances, and it was not possible to measure the resistivity of the samples unless the contacts were placed closer together. This raised the error in the measurements, but was necessary in order to obtain data on all samples. The error in resistivity related to the contact placement and size is on the order of D/L , where D is the diameter of the contact, and L is the length of the sample.⁹ This error was found to be between 7% and 10%.

The films were first fixed to a measurement board. Then contacts were soldered onto the film in the configuration shown in Figure 2-5 c.). The contacts, created using Indium solder, were made as small and uniformly sized as possible. Tungsten wire leads

were then soldered to these contacts. The leads were then attached to the measurement board.

Current is sent through two adjacent contacts, while the voltage is measured across the two contacts opposite those receiving the current, this can be seen in Figure 2-6. This measures the resistance for one configuration of contacts, the equation for this resistance is as follows: $R_{21,34} = V_{34}/I_{21}$.⁹ This equation gives the resistance while current is being pushed from contact 2 to contact 1. By repeating this for every possible configuration of adjacent contacts, as well as reversing the polarity of the current, thermal offsets and other sources of error can be eliminated. The first step is finding the resistance created from each of these different configurations. **Figure 2-6** shows four points labeled with numbers 1-4, as well as the two measurements.

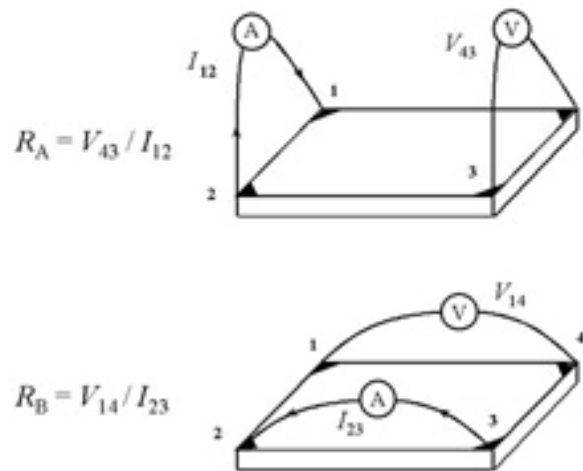


Figure 2-6: Simple method for determining the characteristic resistances of a thin sample.⁹

The resistance that describes one axis (horizontal or vertical) of current flow and voltage measurement is labeled a characteristic resistance. These are found using the following formulas: $R_A = (R_{21,34} + R_{12,43} + R_{43,12} + R_{34,21})/4$, and $R_B = (R_{32,41} + R_{23,14} + R_{14,23} + R_{41,32})/4$.⁹ These resistances are then used to find the resistivity of the sample by

solving the following system of equations: $\exp(-\pi R_A/R_S) + \exp(-\pi R_B/R_S) = 1$, and $\rho = R_S d$.⁹ Where R_S is the sheet resistance measured in Ω , d is the sample thickness, and ρ is the desired resistivity measured in Ωcm . In Figure 2-7 several resistivity measurements are plotted against the substrate temperature. The sharp increase at 350 °C corresponds to the transition from amorphous to the desired polycrystalline films. As temperature increases the resistivity goes down due to the increasing size of grains, or the increased creation of impurities.

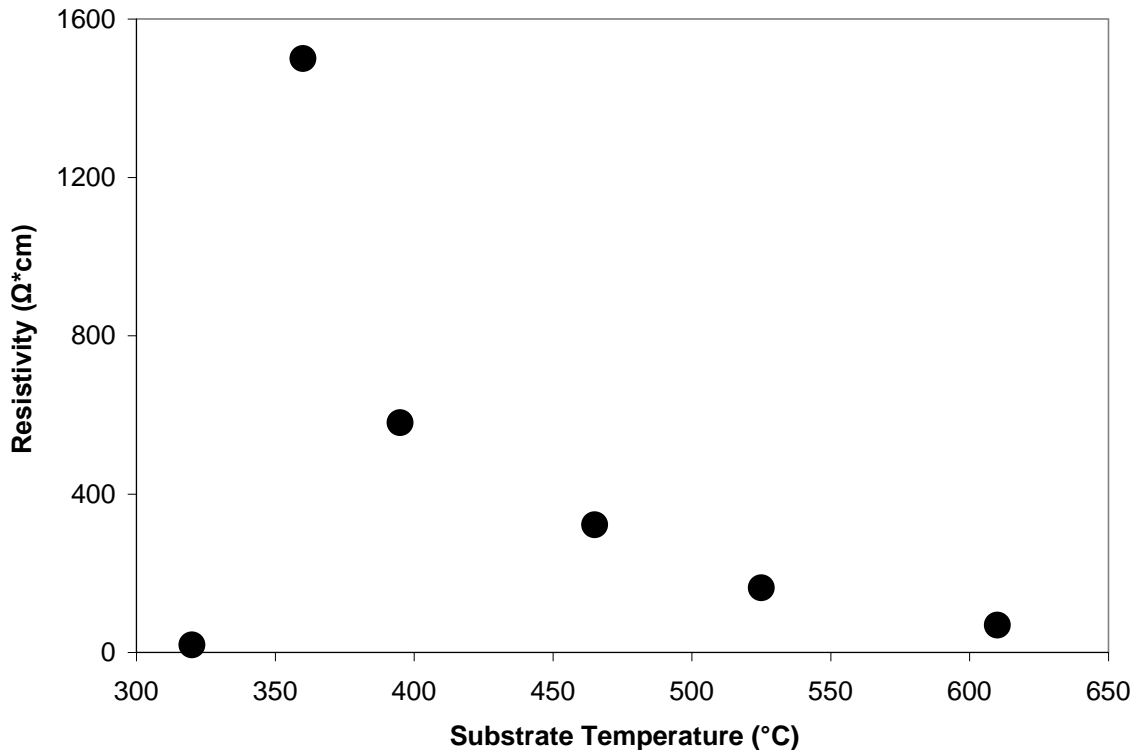


Figure 2-7: Resistivity of BaCuSF thin films deposited at different substrate temperatures.

2.3.2 Seebeck Measurement

The Seebeck coefficient of the samples was measured by placing the sample between two blocks of copper, these served as voltage measuring terminals. A temperature difference, measured by thermocouples was created between the blocks. In

semiconductors, the charge carriers diffuse through the material from the hot side to the cold side. This creates a charge imbalance, as the mobile carriers have moved to one end of the material, while the oppositely charged impurity states are fixed in place. For *p*-type materials the cold side has a higher concentration of holes, while the hot side consists of the bound electrons. This charge imbalance creates a voltage across the material. The voltage reaches equilibrium when the temperature gradient is unable to diffuse additional holes against the created voltage. If the temperature gradient is again increased the voltage would increase in response. This is the basis for the Seebeck coefficient, which gives the change in voltage over the change in temperature. The equation is approximated as: $S = -\frac{\Delta V}{\Delta T}$, where *S* is the Seebeck coefficient. The sign of this coefficient is also very useful, as it provides another means to determine whether a sample is *p*-type, or *n*-type. This is the case because the charges both diffuse in the same direction, thus from the equation above the ΔV switches sign while the ΔT remains the same. A *p*-type semiconductor will yield a positive Seebeck coefficient, while *n*-type will be negative.

In the actual experimental setup, the calculation is not this simple. Since the voltage and temperature are measured from two copper blocks, these must also be accounted for in the calculations. In Figure 2-8 the measured room temperature Seebeck coefficients of several samples are plotted against the deposition temperature. All of the samples show a positive Seebeck coefficient, this shows that the sample is a *p*-type semiconductor.

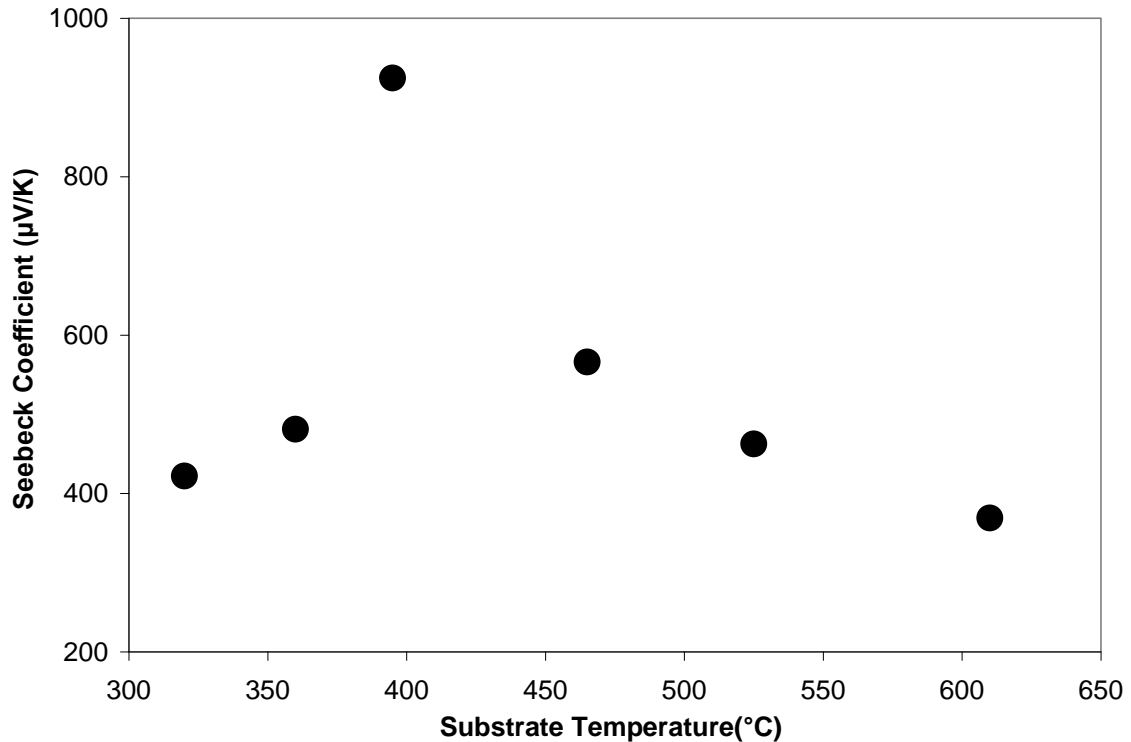


Figure 2-8: Seebeck coefficient measured at different substrate temperatures.

3. PULSED LASER DEPOSITION PARAMETERS

The Pulsed Laser Deposition process has many parameters that can be changed by the user. The system is made up of a laser, and a vacuum chamber. A diagram of the inside chamber can be seen in Figure 3-1. The laser is directed into the vacuum chamber by a series of mirrors and lenses. A dense target of the desired material is placed in the chamber where it is ablated by 20 nanosecond pulses from the laser. The repetition rate of these pulses can be varied from 1 to 10 Hz. The laser fluence is varied around 1 J/cm^2 . This ablation process vaporizes sections of the target, creating plumes of plasma which are incident upon the substrate. The distance between the target and the substrate is varied from 1.5 to 2 inches. The plume strikes the substrate which has a user defined temperature of between 300°C and 600°C , and material is deposited. If the substrate

temperature is high enough, the film will have a crystalline structure. The pressure in the chamber during deposition is typically between 1^{-7} Torr, and 1^{-9} Torr. With the addition of a background gas, such as argon, during deposition this pressure can go as high as 1^{-3} Torr.

The films made during this project used 10000 pulses of BaCuSF. With a deposition rate of 7 Hz, the films took 23 minutes to deposit, and had a thickness of around 200 nm.

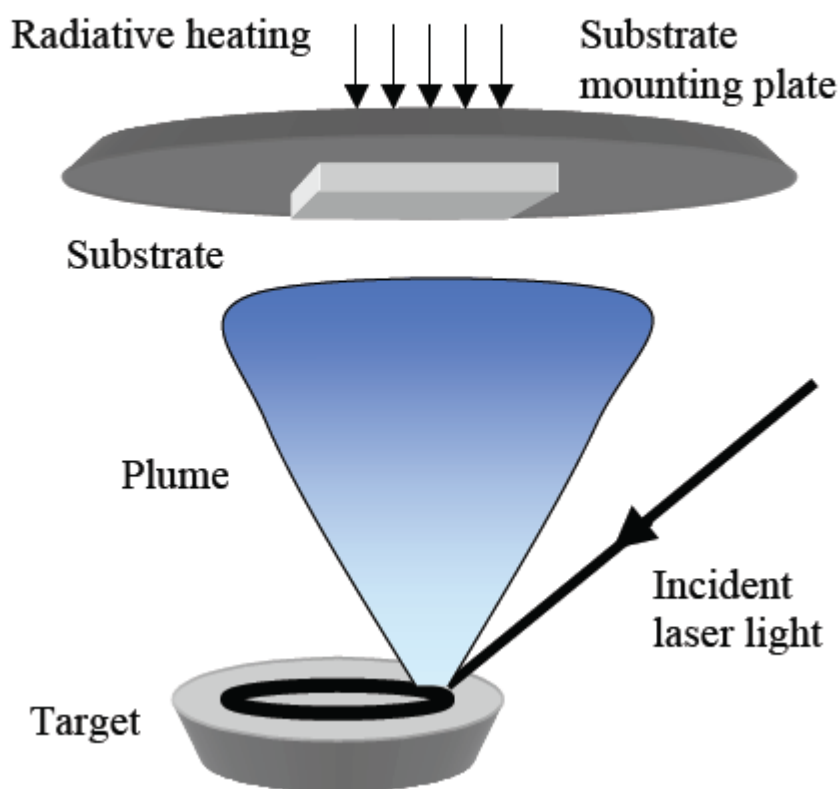


Figure 3-1: Pulsed laser deposition system.

The properties of each film are unique to the deposition parameters that were used. The parameters that result in the biggest changes in film characteristics are:

substrate temperature, repetition rate, target-substrate distance, and background gas pressure.¹⁰ In this experiment, each of these parameters was varied independently and the resulting properties of the films were measured. By varying the parameters, a better idea of how films of BaCuSF respond to the deposition process is gained. The parameters themselves are not always independent of one another, so the knowledge of how different parameters affect one another must be used in order to infer the optimal parameter choice. The desired result is a film that consists of stoichiometry as close to that found in the target as possible. Additionally the film must be as close to a perfect crystalline structure as possible in order for the electrical properties to be good. Each of the varied deposition parameters will be discussed in greater detail in this section.

3.1 Substrate Temperature

Substrate temperature is a critical parameter as the crystal growth is largely determined by this parameter. A quartz lamp heater is placed close to the substrate. This heater uses radiant heating to vary the temperature between 300°C and 650°C. The higher the substrate temperature, the better the atoms are able to diffuse throughout the film in order to find an appropriate placement in the lattice, if the temperature is too high the material can decompose.

At low substrate temperatures, (320°C) it can be seen from the optical measurements that the films are largely amorphous. This amorphous nature is observed in the optical absorption curves in Figure 3-2. The lowest substrate temperature on the absorption curve has no well defined excitonic peak, or band gap.

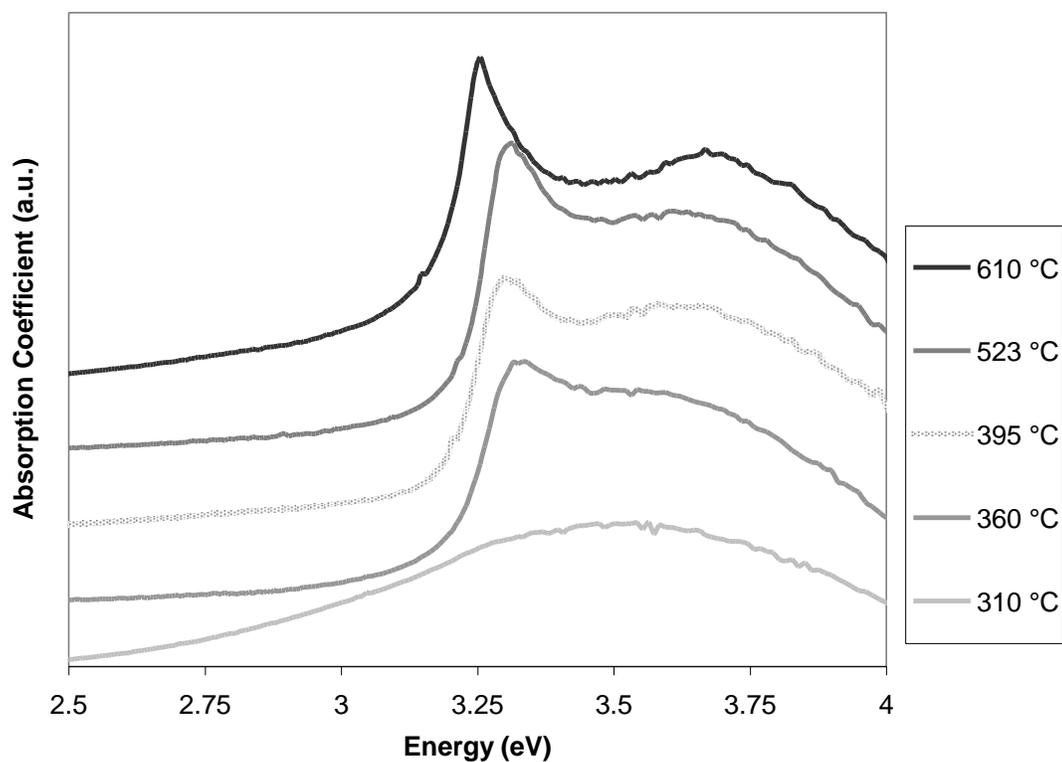


Figure 3-2: Optical absorption graphs of BaCuSF formed at different substrate temperatures. For easier viewing the graphs have been offset vertically.

The XRD results in Figure 3-3 show the peaks corresponding to the film grown at 320°C are not as sharp as those for the higher temperatures. This shows that the films have not formed well defined crystal structures, and also supports the optical measurements.

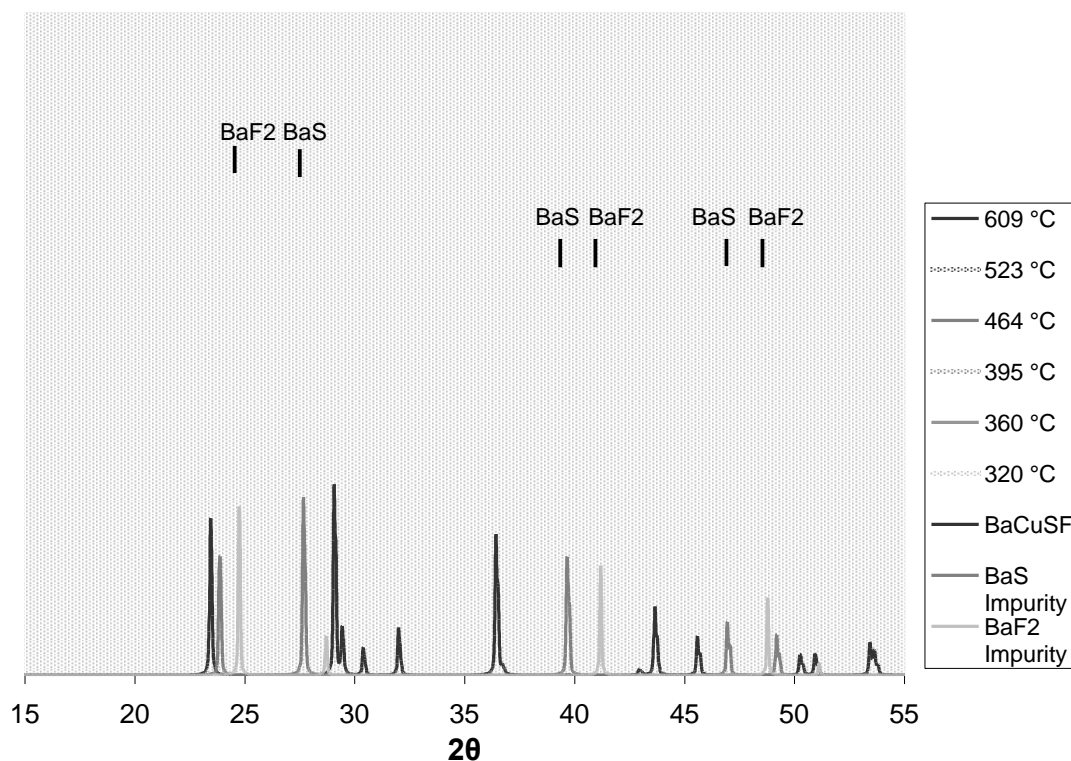


Figure 3-3: X-ray diffraction patterns of BaCuSF films formed at different substrate temperatures.

The XRD powder spectra of BaCuSF, BaF₂, and BaS are shown for comparison

As the temperature is increased, improvements in the film quality can be seen as a sharpening of the excitonic peaks in Figure 3-2, and also a sharpening of the peaks in the x-ray diffraction patterns. This improvement in optical qualities is due in large part to the improvement of the crystal structure. Up to 525°C the film characteristics are improved with no addition of impurities to the material. At the highest temperature tested, 610°C, additional phases, which include BaF₂ and BaS, begin to form. These impurities can be seen from peaks in the film pattern that match their individual XRD patterns. These defects begin to form because at high temperatures these phases are the optimal formations for the material.

The measurements taken show that the best film quality is achieved at a deposition temperature of 525 °C.

3.2 Target-Substrate Distance

The target-substrate distance determines the distance that particles in the plume must travel in order to reach the substrate. This distance is important because it alters the kinetic energy of the particles reaching the substrate. Particles may also be scattered out of the plume with an increased distance.¹⁰ Two different target-substrate distances are used, 2" and a 1.5". The 2" distance was chosen because the X-ray diffraction pattern, in Figure 3-4, shows much better quality. The BaCuSF peaks are sharper and no impurity peaks exist for the film deposited 2 inches from the substrate. While the film deposited 1.5 inches from the substrate show numerous impurity peaks.

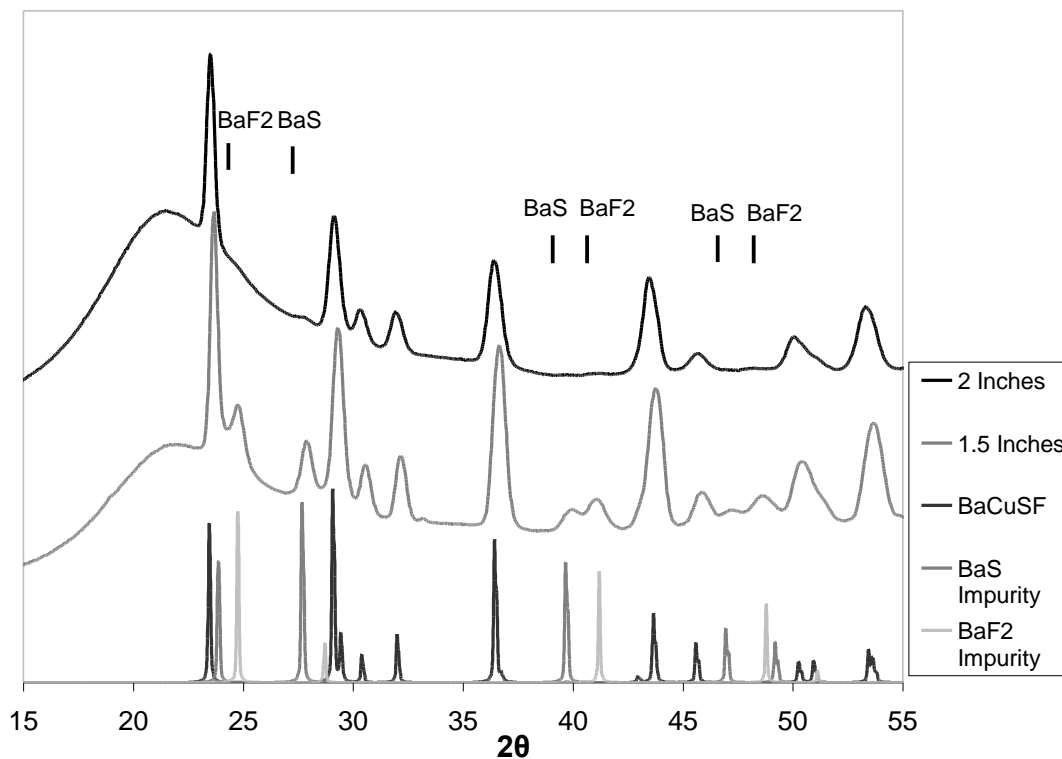


Figure 3-4: X-ray diffraction patterns of BaCuSF films formed at different target-substrate distances. The XRD powder spectra of BaCuSF, BaF₂, and BaS are shown for comparison.

3.3 Repetition Rate

The repetition rate affects the time which the deposited material has to orient itself into the structure. The rate must be low enough to allow for this re-orientation. But the rate cannot be too low to allow for additional reactions to occur.¹⁰ The rates that were compared are 7 Hz, 3Hz, and 1Hz. The XRD data in Figure 3-5 shows that a repetition rate of 3 Hz results in the sharpest XRD peaks as well as the fewest, and smallest impurity peaks.

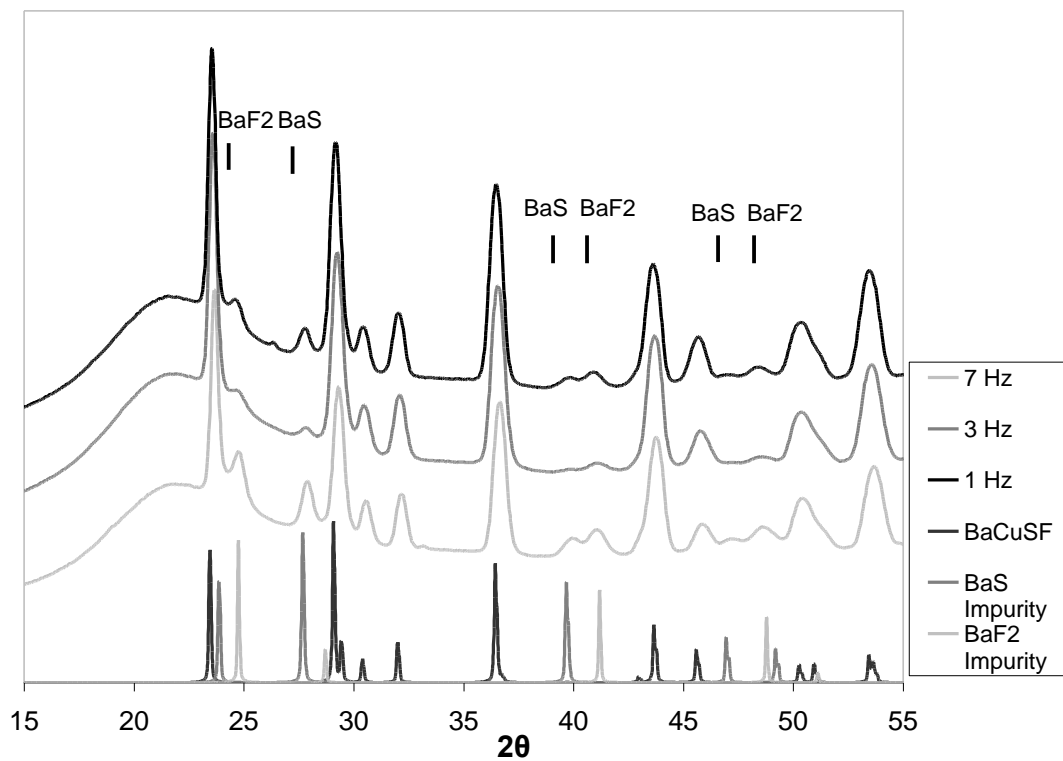


Figure 3-5: X-ray diffraction patterns of BaCuSF films formed using different laser repetition rates.

The absorption curves shown in Figure 3-6 also support a deposition rate of 3 Hz, with this curve having the sharpest excitonic peak.

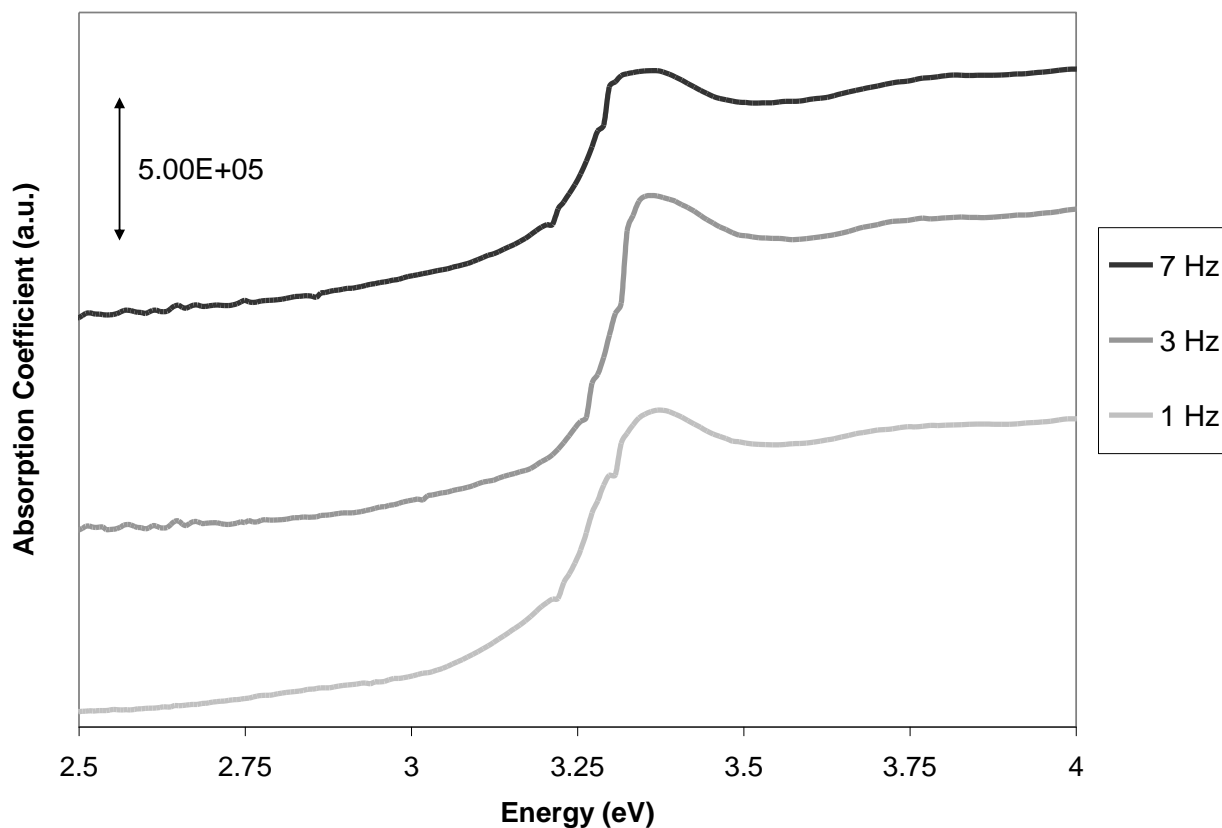


Figure 3-6: Optical absorption graphs of BaCuSF formed at varying laser repetition rates. The graphs have been offset vertically.

3.4 Background Gas Pressure

The background gas pressure affects the plume by having particles in the plume collide with the background gas particles, which lowers the kinetic energy of the plume particles. This affects the smaller particles more than the larger particles, as they begin with a lower kinetic energy. Argon is used as the background gas due to its inert nature. Figure 3-7 shows that at argon pressure of 10^{-3} Torr the film quality is very low. There are many impurity peaks and the peaks corresponding to BaCuSF are not as sharp.

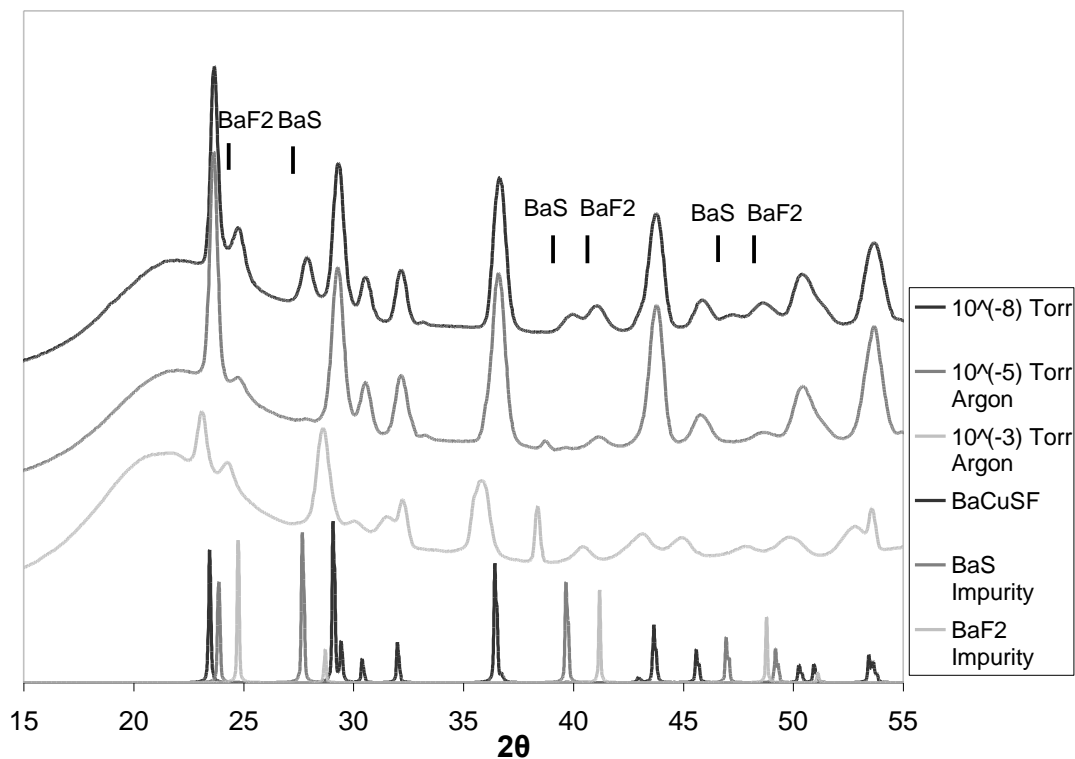


Figure 3-7: X-ray diffraction patterns of BaCuSF films formed using different background gas pressures.

The film produced with no Argon gas has a background pressure of 10^{-8} Torr. This film had fewer impurity peaks, and sharper BaCuSF peaks than the film deposited at an Ar pressure of 10^{-3} Torr. The film with the best qualities was that deposited at an Ar background pressure of 10^{-5} Torr. This conclusion is also supported by the optical data seen in Figure 3-8. The sharpest excitonic peak is observed in the film produced at 10^{-5} Torr of background argon pressure.

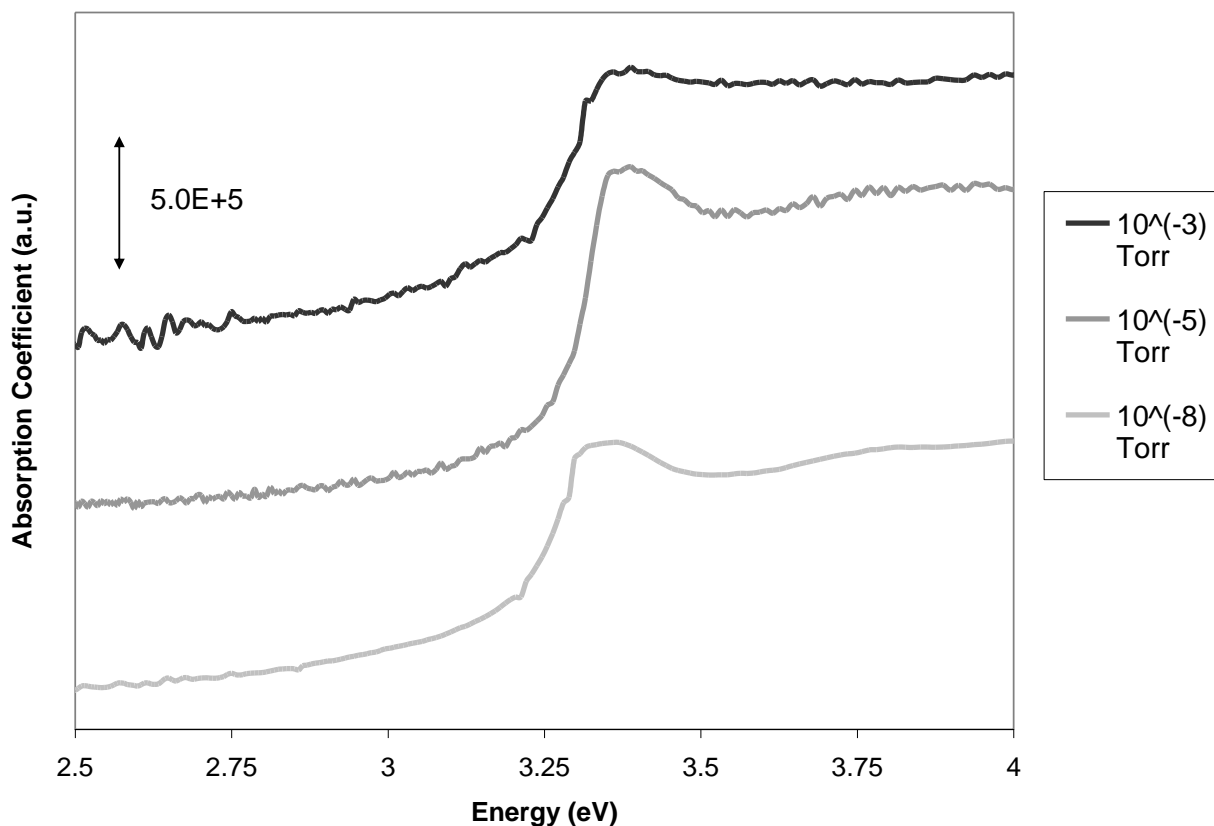


Figure 3-8: Optical absorption graphs of BaCuSF formed at varying background gas pressures, at 525°C substrate temperature, .

4. COPPER DOPING

Copper is introduced in the films by intermittently adding pulses from a copper target to the substrate. The copper is added by switching the targets between a CuBaSF target to a pure copper target. Several pulses from this copper target are added to the film at intervals of 1000 pulses of BaCuSF. By adding extra copper to the films, the number of copper vacancies is expected to decrease. It is expected that these intermittent pulses of copper will diffuse throughout the film, filling copper vacancies in the crystal lattice. This should in principle lead to higher resistivity in the samples.

The successful diffusion of the copper as well as the overall film quality is characterized using the methods described earlier. These characterizations allow the films deposited with copper to be compared to those without copper, and conclusions will be drawn from the results. It is expected from electron probe micro-analyzer (EPMA) data taken on films of BaCuTeF that the amount of added copper is proportional to the number of pulses of copper. By fitting a trend to the results obtained from EPMA on BaCuTeF an estimate for the amount of copper present in the films of BaCuSF is achieved. These estimates can be seen in Figure 4-1.

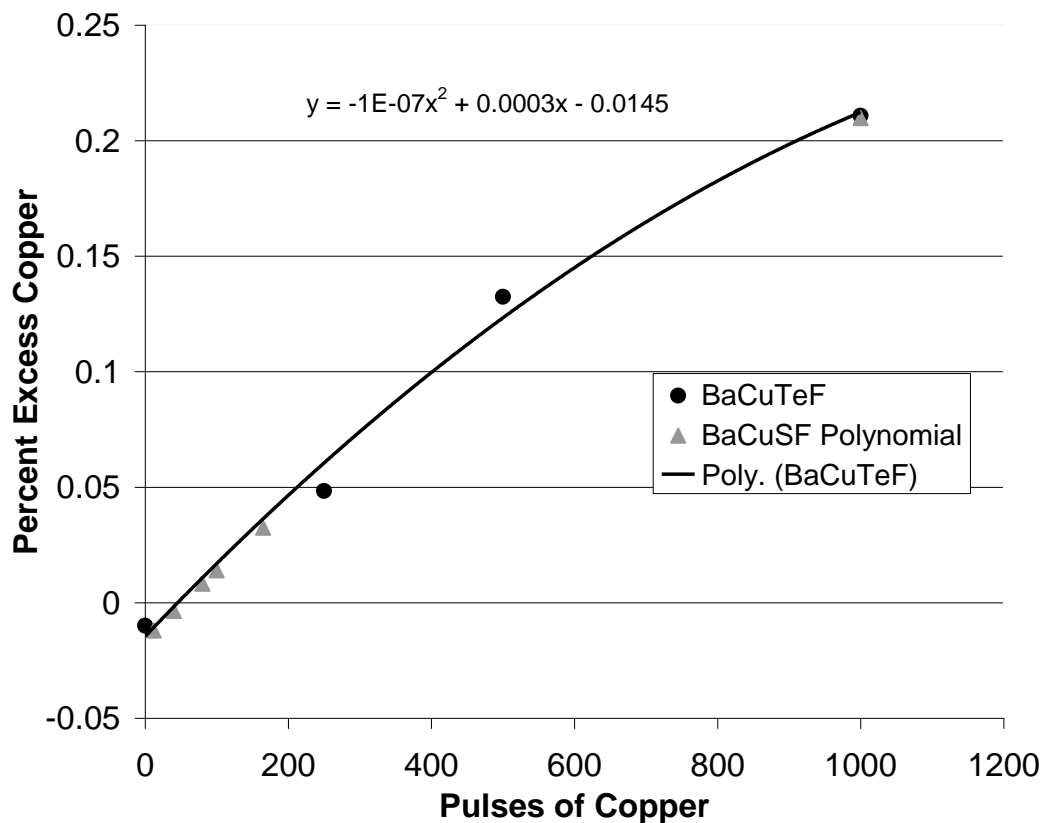


Figure 4-1: Amount of excess copper present in films of BaCuSF. Amount is extrapolated from previous EPMA data gathered on BaCuTeF.

The film created with 12 pulses of copper is found to be 1.2% copper deficient, this relates to a slight decrease in copper deficiency from what is found with no copper. The film created with 40 pulses is predicted to be 0.3% copper deficient. This is the closest film to stoichiometry. The films then gain more copper up to 20% copper excess in the film created with 1000 pulses.

The pulses of copper range from 12 – 1000, this is in addition to the 10000 pulses of BaCuSF used in the films. First the structural characteristics of the material will be explored. The X-ray diffraction patterns for the measured films with added copper correspond very well with the reference pattern. Figure 4-2 shows that none of the impurity peaks are as sharp as those found while varying the deposition parameters. The XRD graph for zero pulses of copper is very good since the parameters have been optimized for this. For 160 pulses of copper, the film quality is the same as with zero pulses of copper, with no impurity peaks. For all the rest of the films with added copper, 80, 100, and 1000, BaF₂ and BaS impurity peaks become visible. The impurity peaks visible at 1000 pulses of copper, are slightly larger than those seen in the other patterns. This might be caused by the additional copper interacting with the material and creating impurities. The XRD data done on the films with 12 pulses and 40 pulses was taken a significant time after deposition (1 year). The data on these films show lower film quality than on most of the other films. These results do cast some doubt on the idea that copper is filling vacancies at these low levels. Due to the inconsistency of time delay until measurement between the films, these two films will neither prove nor disprove the current hypothesis.

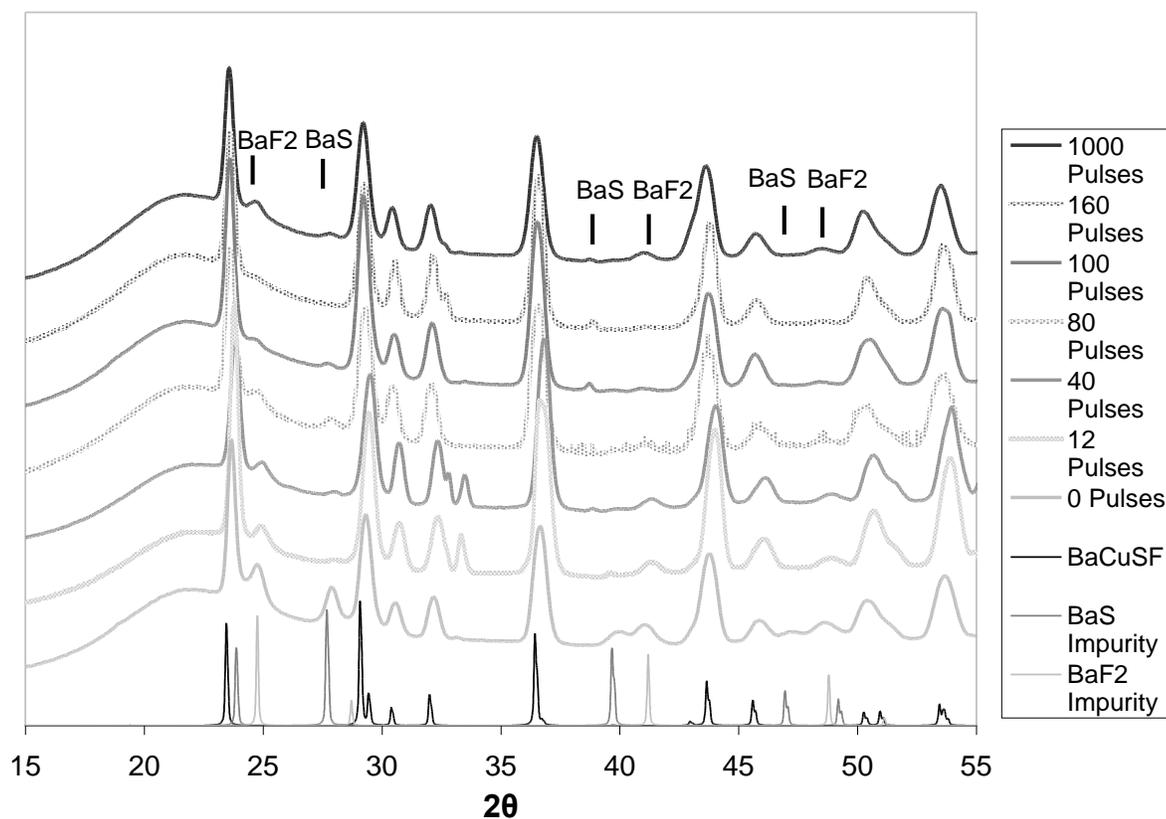


Figure 4-2: XRD results for BaCuSF films doped with various amounts of excess copper, deposited using optimal parameters. The samples with 12 and 40 pulses were measured significantly later than the other films.

It is found that the structural characteristics of the films produced with copper are relatively similar, but of slightly lower quality than those produced without copper but with the same deposition parameters. This can be seen more definitively in Figure 4-3, absorption vs. copper content. The film with no copper has a sharper excitonic peak, and the area before the peak has less absorption, while the films with copper get worse with additional copper.

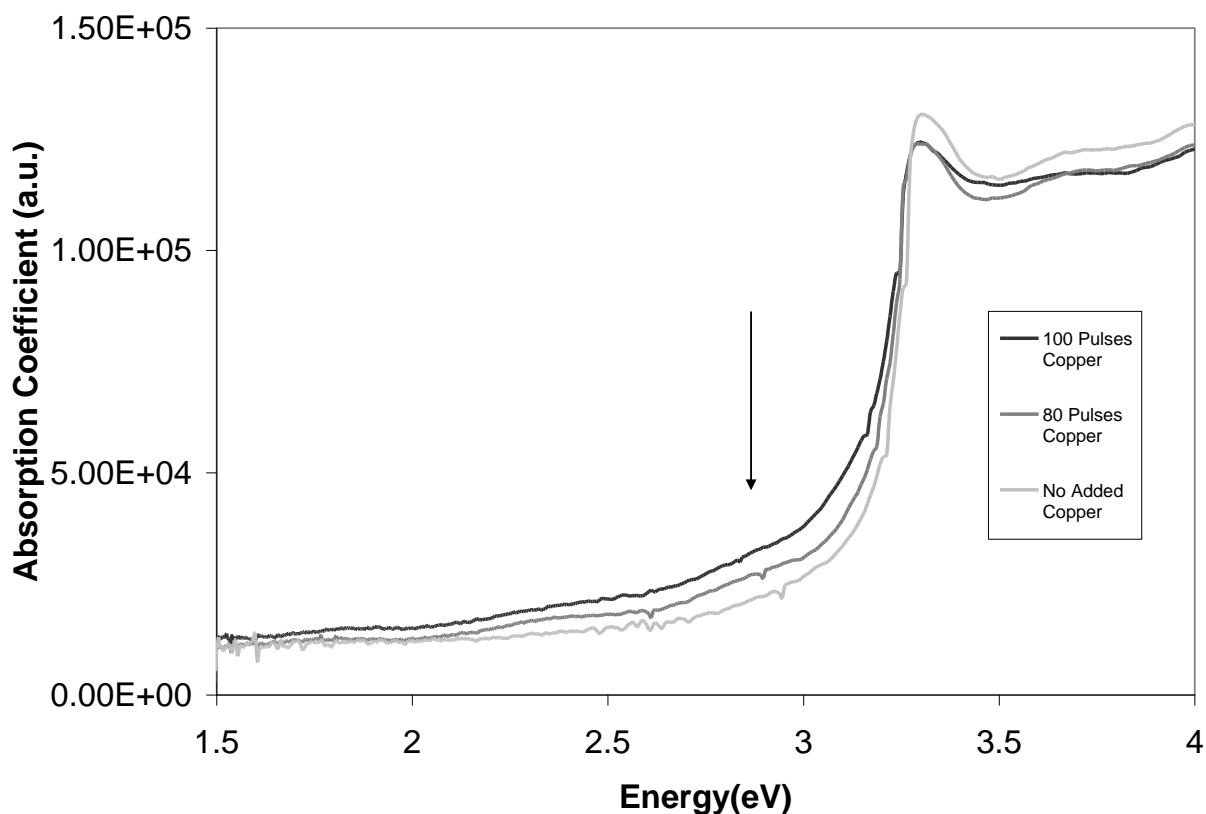


Figure 4-3: Optical absorption in BaCuSF thin films with varying amounts of added copper, deposited using optimal parameters.

By adding extra copper to the films, the number of copper vacancies is expected to decrease. This should in principle lead to higher resistivity in the samples. It can be seen in the resistivity measurements in Figure 4-4 that the resistivity does indeed increase to a maximum and then comes back down to below its original value. This is interesting as the resistivity change is not mirroring any impurity, or quality trends found in the structural measurements. This would tend to indicate that the change in resistivity is due to some internal mechanism such as the filling of copper vacancies.

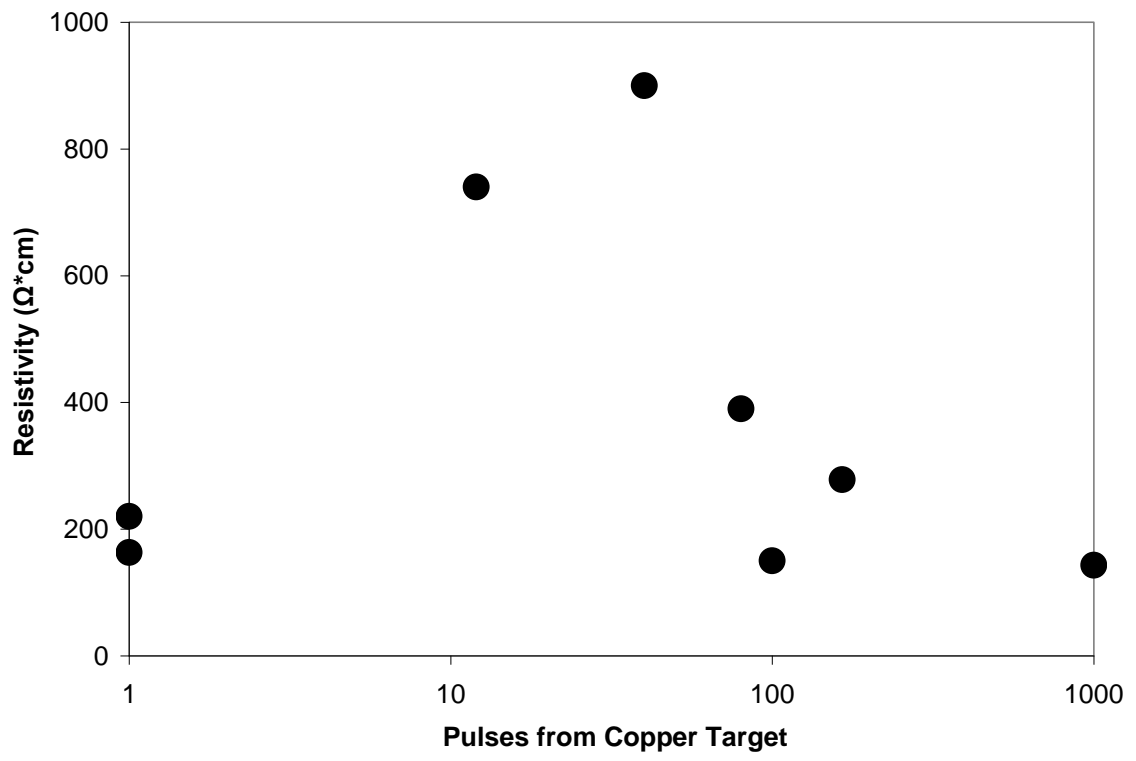


Figure 4-4: Resistivity measured for varying amounts of added copper.

The overall decrease in resistivity from zero pulses of copper to 1000 pulses of copper could be due to the created impurities. The increase in resistivity observed between 12 pulses and 80 pulses supports the claim that copper vacancies are indeed being filled.

5. CONCLUSION

In this paper the optimal deposition parameters for BaCuSF were found using various characterization techniques. The optimal deposition parameters were found to be the following: a substrate temperature of 525 °C, an Argon gas pressure of 10^{-5} Torr, a target substrate distance of 2 inches, and a pulse repetition rate of 3 Hz. Using these deposition parameters excess copper was added to the samples. For small amounts of added copper, 12 pulses and 40 pulses, the resistivity rose significantly, from 200 Ωcm , to 740 Ωcm and 900 Ωcm respectively. The optical measurements and the XRD patterns show that these films have the same quality as the films produced at optimal deposition parameters with no added copper. The estimate of the amount of copper added based on EPMA results taken on BaCuTeF predicts that 40 pulses of excess copper would fill the copper vacancies present in the material. The good optical and XRD results, combined with the agreement with the amount of excess copper needed to fill the vacancies yields good confidence in this result.

For greater amounts of copper, 80 pulses to 1000 pulses, the resistivity decreases back to around 200 Ωcm . The films with higher amounts of copper also show lower quality in optical measurements, and XRD begins to show addition of BaS, and BaF₂. This shows that copper added beyond 40 pulses no longer fills copper vacancies. This added copper is free to interact with the other atoms present in the material. These interactions form impurities in the film, which cause the resistivity to lower. Unfortunately the two most important films those with 12, and 40 pulses of copper did not have XRD data taken on them until well after the other films were characterized. Once measured these films both yielded high impurity levels. It is unknown if these

impurities were there upon deposition or if they were introduced during the time between deposition and measurement.

These experiments leave many questions however. There exist many regions to explore in this data. Additional samples must be deposited with the number of pulses of copper varied only slightly. This needs to be done because additional data points are necessary in order to prove the relationship between added copper and resistivity. EPMA data must be taken on the BaCuSF samples. This will increase the confidence in the amount of copper present in the samples. In order to gain more insight from the resistivity measurements it would be helpful to have the capability of measuring the mobility and carrier concentration of the samples. These measurements were unable to be taken due to the high resistance of the samples? With these added measurements it would be possible to make much stronger conclusions. Matching increasing excess copper with decreasing carrier concentration would be strong evidence of the copper vacancy filling phenomenon.

Using single-crystals in order to characterize BaCuSF could be another promising route. Single-crystals are relatively defect free, and would allow additional measurements to be taken. For CuAlO₂ very reliable, and reproducible measurements were taken on single-crystals of this material.¹¹ This same quality of measurements is also likely in BaCuSF taken on single-crystals.

6. BIBLIOGRAPHY

- ¹ H. Yanagi, J. Tate, S. Park, C.-H. Park, D. Kezler, Appl. Phys. Lett. 82 (2003) 17
- ² Department of Materials Science, University of Illinois, Scientific Principles <http://matse1.mse.uiuc.edu/sc/prin.html> (2003)
- ³ H. Raebiger, S. Lany, and A. Zunger, Phys. Rev. B 76, 045209, (2007)
- ⁴ R. Kykyneshi, Phd thesis, Oregon State University, (2007), Pg. 3-5
- ⁵ E.A.Radzhabov, A.I.Nepomnyashikh, Proceedings of The Fifth International Conference on Inorganic Scintillators and Their Applications, 1999
- ⁶ R. Kykyneshi, Phd thesis, Oregon State University, (2007), Pgs. 4
- ⁷ A Zakutayev, private communication (2009)
- ⁸ Optics 4th Ed., Ch. 4, E. Hecht, Pearson Education, Inc. (2002)
- ⁹ NIST, Standard Reference Materials, www.nist.gov
- ¹⁰ Pulsed Laser Deposition of Thin Films, Ch. 9, Edited by Douglas B. Chrisey and Graham K.
- ¹¹ J. Tate, H.L. Ju, J.C. Moon, A. Zakutayev, A.P. Richard, J. Russel, and D.H. McIntyre, Origin of p-type conduction in single crystal CuAlO₂, submitted to Phys. Rev. B